

# Doping-driven Mott transition in $\text{La}_{1-x}\text{Sr}_x\text{TiO}_3$ via simultaneous electron and hole doping of $t_{2g}$ subbands

A. Liebsch

*Institut für Festkörperforschung, Forschungszentrum Jülich, 52425 Jülich, Germany*

(Dated: February 5, 2020)

The insulator to metal transition in  $\text{LaTiO}_3$  induced by La substitution via Sr is studied within multi-band exact diagonalization dynamical mean field theory at finite temperatures. It is shown that weak hole doping triggers a large interorbital charge transfer, with simultaneous electron and hole doping of  $t_{2g}$  subbands. The transition is first-order and exhibits phase separation between insulator and metal. In the metallic phase, subband compressibilities become very large and have opposite signs. Electron doping gives rise to an interorbital charge flow in the same direction as hole doping. These results can be understood in terms of a strong orbital depolarization.

DOI: 10.1103

PACS numbers: 71.10.Fd, 71.27.+a, 71.30.+h

The remarkable sensitivity of the electronic and magnetic properties of transition metal oxides to small changes of parameters such as temperature, pressure, or impurity concentration has attracted wide attention during recent years [1]. A phenomenon of particular interest is the filling-controlled metal insulator transition in the vicinity of integer occupancies of partially filled valence bands. For instance,  $\text{LaTiO}_3$  is known to be a Mott insulator which becomes metallic if La is replaced by a few percent of Sr ions [2, 3]. This kind of doping-driven insulator to metal transition has been discussed theoretically in terms of single-band models [4, 5, 6, 7, 8, 9, 10, 11, 12, 13] or multi-band models based on degenerate orbitals [14, 15, 16]. To our knowledge, only one calculation for non-identical subbands exists so far [17].

It has recently been shown that orbital degrees of freedom play a crucial role in the Mott transition of materials consisting of non-equivalent partially occupied subbands. For example, whereas cubic  $\text{SrVO}_3$  ( $3d^1$  configuration) is metallic, iso-electronic  $\text{LaTiO}_3$  exhibits a Mott transition because non-cubic structural distortions lift the degeneracy among  $t_{2g}$  subbands [18]. Local Coulomb interactions strongly enhance this orbital polarization, so that the electronic structure of the insulating phase consists of a single nearly half-filled band split into lower and upper Hubbard peaks, and two nearly empty  $t_{2g}$  subbands. Similarly, the monoclinic symmetry of the Mott insulator  $\text{V}_2\text{O}_3$  ( $3d^2$ ) yields a pair of nearly half-filled subbands (with lower and upper Hubbard peaks) and a single nearly empty  $t_{2g}$  band [19, 20]. Also, the insulating phase of the layered perovskite  $\text{Ca}_2\text{RuO}_4$  ( $4d^4$ ) consists of a fully occupied  $t_{2g}$  band of predominant  $d_{xy}$  character and two half-filled  $d_{xz,yz}$ -like bands [21]. In view of the nearly complete orbital polarization of the Mott phase of these systems it is evidently necessary to go beyond single-band or degenerate multi-band models to describe the effect of electron or hole doping.

In the present paper we investigate the destruction of the Mott phase of  $\text{LaTiO}_3$  due to replacement of small amounts of La by Sr. To account for the orbital degrees of freedom during hole doping we make use of a

recent multi-band extension of dynamical mean field theory based on exact diagonalization [22]. This approach has been shown to be highly useful for the study of strong correlations in several transition metal oxides [21, 22, 23]. Since it does not suffer from sign problems the full Hund exchange including spin-flip and pair-exchange contributions can be taken into account. Also, relatively large Coulomb energies and low temperatures can be reached.

Naively, one might expect that all subbands are affected similarly by the doping process, perhaps weighted by their relative occupancies. The result of this work is a completely different picture. As we show below, the addition of only a few percent of holes in the  $t_{2g}$  bands triggers a substantially larger interorbital charge rearrangement, with a strong flow of electrons from the nearly half-filled subband towards the nearly empty ones. In other words, weak “external” hole doping of the  $t_{2g}$  bands causes a much larger “internal” simultaneous electron and hole doping of different subbands. Thus, the density-driven insulator to metal transition in  $\text{La}_{1-x}\text{Sr}_x\text{TiO}_3$  is accompanied by a significant reduction of orbital polarization. We also show that electron doping of the  $t_{2g}$  bands, which could be achieved by substitution of La by Zr, leads to a strong charge flow in the same direction as hole doping, i.e., from the nearly half-filled  $t_{2g}$  band to the nearly empty ones.

As shown by Pavarini *et al.* [18], the octahedral distortions due to the orthorhombic lattice of  $\text{LaTiO}_3$  ensure that the  $t_{2g}$  density of states is not diagonal within the  $xy, xz, yz$  basis. It is nonetheless possible to construct from the  $t_{2g}$  orbitals a new basis which is nearly diagonal [24]. We denote this basis here as  $a_g$  and  $e'_g$ . The corresponding densities of states obtained from *ab initio* calculations within the local density approximation (LDA) are shown in Fig. 1. The centroid of the  $a_g$  density lies about 200 meV below that of the two nearly degenerate  $e'_g$  contributions. Accordingly, the subband occupancies (per spin band) in the absence of correlation effects are  $n_a \approx 0.23$  and  $n_e \approx 0.135$ . This  $t_{2g}$  crystal field splitting compares well with recent experimental estimates based on X-ray studies [25, 26].

To account for local Coulomb interactions among the

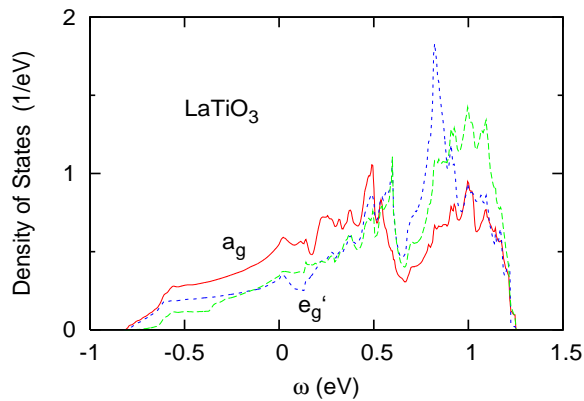


FIG. 1: (Color online) Density of states components of  $\text{LaTiO}_3$  in nearly diagonal  $t_{2g}$  subband representation [24]. Solid (red) curve:  $a_g$  states, dashed (blue and green) curves:  $e'_g$  states;  $E_F = 0$ .

Ti  $3d$  electrons we use finite temperature dynamical mean field theory (DMFT) [27, 28, 29, 30] combined with exact diagonalization (ED) [31]. It was recently shown [22] that this method can be generalized to multi-band materials by computing only those excited states of the impurity Hamiltonian that are within a narrow range above the ground state, where the Boltzmann factor provides a suitable convergence criterion. In the present case, each of the three  $t_{2g}$  impurity orbitals couples to two bath levels, giving a cluster size  $n_s = 9$  with maximum Hamiltonian dimension 15.876. Exploiting the sparseness of the impurity Hamiltonian, a limited number of excited states can be computed very efficiently by using the Arnoldi algorithm [32]. Since local Coulomb and exchange interactions couple the baths of the three  $t_{2g}$  orbitals, the level spacing between excited states is very small so that finite size effects are much smaller than for a single impurity level coupled to only two bath levels.

Fig. 2 shows the variation of the  $a_g$  and  $e'_g$  subband occupancies with Coulomb energy. Full Hund exchange is included, and the exchange energy is held fixed at  $J = 0.65$  eV [18]. The inter-orbital Coulomb energy is given by  $U' = U - 2J$ . The temperature is  $T = 10 \dots 20$  meV. For simplicity, the small difference between the  $e'_g$  densities is neglected and their average density is used instead. Integer and non-integer occupancy are seen to lead to qualitatively different behavior. For  $n = 2n_a + 4n_e = 1$ , local Coulomb interactions gradually suppress orbital fluctuations up to  $U \approx 4.5$  eV. In the subsequent narrow range up to  $U = 5.0$  eV, the  $a_g$  band is rapidly becoming nearly half-filled and the two  $e'_g$  bands nearly empty. This result supports the picture presented in Refs. [18, 24], where for  $U = 5.0$  eV, Ising exchange, and  $T = 100$  meV,  $\text{LaTiO}_3$  was found to be a Mott insulator, with nearly empty  $e'_g$  subbands, and the half-filled  $a_g$  band split into lower and upper Hubbard peaks [33].

For hole doping with  $n = 0.95$  and  $0.90$ , on the other

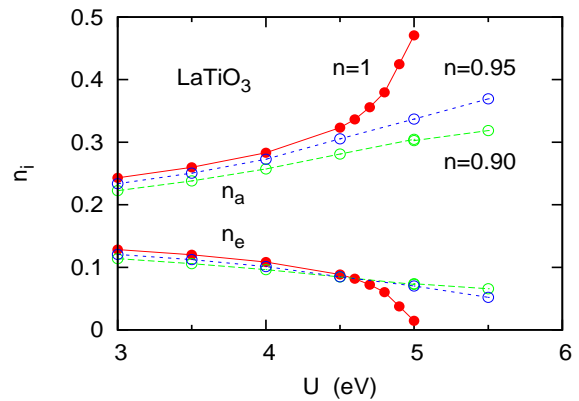


FIG. 2: (Color online) Subband occupancies (per spin band) of  $\text{La}_{1-x}\text{Sr}_x\text{TiO}_3$  as functions of Coulomb energy. Solid (red) curves:  $3d^1$  ( $x = 0$ ); dashed (blue) curves:  $3d^{0.95}$  ( $x = 0.05$ ); long-dashed (green) curves:  $3d^{0.90}$  ( $x = 0.1$ ).

hand, the orbital polarization increases smoothly with increasing Coulomb energy, without any sign of the critical behavior that is characteristic of the pure La compound. Evidently, the rapid suppression of orbital fluctuations near  $U = 5.0$  eV is a phenomenon associated with the integer occupancy of the  $t_{2g}$  bands. To illustrate the destruction of the Mott phase of  $\text{LaTiO}_3$  via doping with Sr we assume here that the primary effect is caused by the change of band filling. Additional modifications of the  $a_g$  and  $e'_g$  density of states due to the slightly smaller size of Sr compared to La are neglected.

The unexpected and striking feature of these results is that the charge rearrangement among  $t_{2g}$  orbitals is much larger than the number of holes induced via La  $\rightarrow$  Sr substitution. For instance, for  $x = 0.05$  ( $n = 0.95$ ) the total  $a_g$  occupancy (both spins) changes from near unity to 0.64, whereas the total  $e'_g$  occupancy (four spin bands) changes from near zero to 0.31. Thus, the internal charge transfer from  $e'_g$  to  $a_g$  bands is six times larger than the external charge transfer due to doping with Sr. Clearly, the destruction of the Mott phase of  $\text{LaTiO}_3$  via hole doping does not proceed via approximately equal participation of all subbands. Instead, weak external hole doping generates a much larger simultaneous electron and hole doping in different  $t_{2g}$  subbands.

Since the density of states of  $\text{LaTiO}_3$  is not symmetric and the  $t_{2g}$  occupation is far from one-half, it is interesting to consider also the case of electron doping, for example, via substituting La by Zr. Because the  $a_g$  band is nearly full, one might expect the donated electrons to populate the nearly empty  $e'_g$  bands, with little other changes. As in the hole doping case, we find an entirely different picture. For example, for 0.10 electron doping, 0.26 electrons are injected into the  $e'_g$  bands and 0.16 holes into the  $a_g$  band. Thus, the actual number of electrons transferred to the  $e'_g$  bands is 2.6 times larger than externally supplied. Of course, this can only be achieved via simultaneous hole doping of the nearly filled  $a_g$  band.

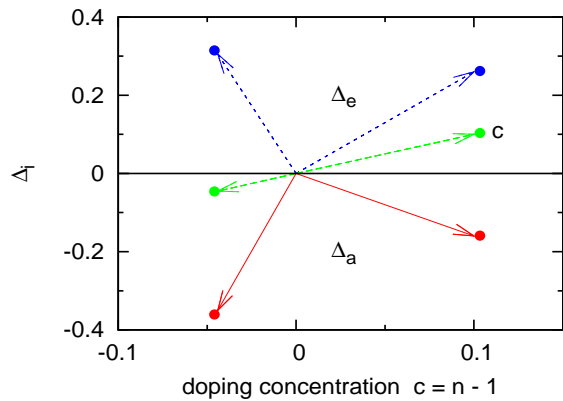


FIG. 3: (Color online) Red and blue dots: doping induced change of total  $a_g$  and  $e'_g$  subband occupancies,  $\Delta_a$  and  $\Delta_e$ , respectively, for hole doping ( $c \approx -0.05$ ) and electron doping ( $c \approx 0.1$ );  $U = 5.0$  eV. In both cases, holes are injected into the nearly half-filled  $a_g$  band (red arrows) and electrons into the nearly empty  $e'_g$  bands (blue arrows). The green arrows denote the net doping.

These results are illustrated in Fig. 3 which shows the total electronic charge injected into the  $e'_g$  bands ( $\Delta_e = 4n_e > 0$ ) and the total hole charge injected into the  $a_g$  bands ( $\Delta_a = 2n_a - 1 < 0$ ) for net doping concentrations  $c \approx -0.05$  and  $c \approx 0.1$ , where  $c = \Delta_a + \Delta_e = n - 1$ . Both electron and hole doping are seen to cause a strong orbital depolarization, implying an internal charge flow between  $t_{2g}$  bands that is significantly larger than the externally supplied number of electrons or holes. Note also the lack of symmetry between electron and hole doping.

Fig. 4 shows in more detail the charge transfer among  $t_{2g}$  bands as a function of chemical potential. The Coulomb and exchange energies are held constant at values appropriate for  $\text{LaTiO}_3$ . Hole doping occurs for  $\mu < 1.5$  eV, electron doping for  $\mu > 2.5$  eV. Because of the insulating gap, the charge compressibility  $\kappa = \partial n / \partial \mu$  vanishes in the intermediate range, i.e., the chemical potential can be varied without changing the subband occupancies. The small deviations from  $n_a = 0.5$  and  $n_e = 0.0$  in this region presumably are due to the finite temperature and ED finite size effects. The hysteresis loops near  $\mu = 1.5$  eV and  $\mu = 2.5$  eV demonstrate that the hole and electron driven Mott transitions at finite  $T$  are first order. Phase separation, where an insulating solution with  $n = 1$  coexists with a metallic solution for  $n \neq 1$ , is seen to occur at both transitions. Moreover, the compressibility gets very large as the upper and lower critical values of  $\mu$  at both loops are approached. Note that the hysteresis behavior of the  $a_g$  and  $e'_g$  subbands is much more pronounced than that of the average  $t_{2g}$  charge. Accordingly, the subband compressibilities  $\kappa_i = \partial n_i / \partial \mu$  have opposite signs and their absolute values are much larger than the average  $t_{2g}$  compressibility. These results show that the orbital degrees of freedom lead to a non-trivial generalization of the one-band picture close to half-filling [4, 5, 6, 7, 8, 9, 10, 11, 12, 13] and of the multi-

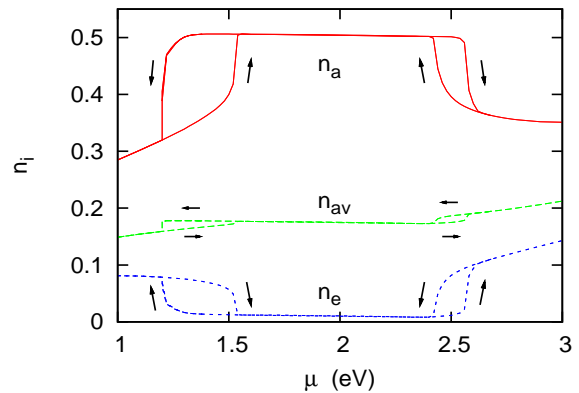


FIG. 4: (Color online) Solid (red) and dashed (blue) curves:  $a_g$  and  $e'_g$  subband occupancies (per spin band) of  $\text{LaTiO}_3$  as functions of chemical potential for  $U = 5.0$  eV. Long-dashed (green) curve: average occupancy  $n_{av} = (n_a + 2n_e)/3$ .  $\mu < 1.5$  eV corresponds to hole doping,  $\mu > 2.5$  eV to electron doping. The arrows mark the hysteresis behavior for increasing and decreasing  $\mu$ , indicating the first-order nature of the density-driven Mott transition.

band picture based on equivalent orbitals [14, 15, 16].

Finally, to make contact with the photoemission data for  $\text{La}_{1-x}\text{Sr}_x\text{TiO}_3$  [3], we show in Fig. 5 the quasi-particle spectra for  $n = 1$  ( $x = 0$ ) and  $n = 0.95$  ( $x = 0.05$ ). For simplicity, we give here the ED cluster spectra which can be evaluated directly at real  $\omega$ , without requiring extrapolation from Matsubara frequencies. At integer occupancy the system is insulating. The excitation gap is formed between the lower Hubbard peak of the  $a_g$  band

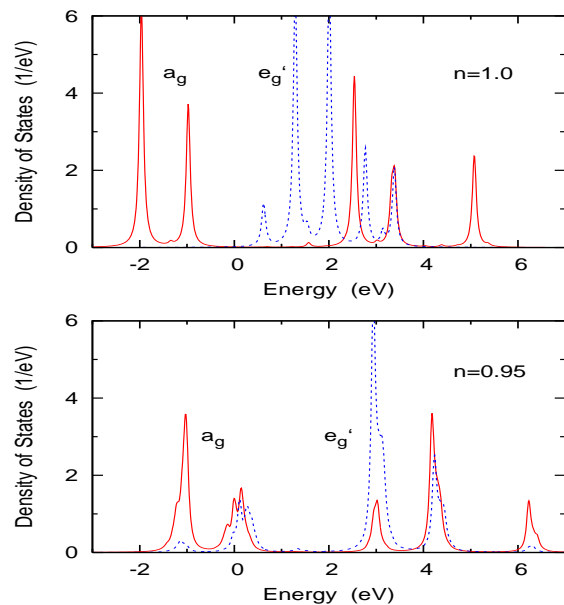


FIG. 5: (Color online) Quasi-particle spectra of  $\text{LaTiO}_3$  (upper panel) and  $\text{La}_{0.95}\text{Sr}_{0.05}\text{TiO}_3$  (lower panel) for  $U = 5$  eV. Solid (red) curves:  $a_g$  states, dashed (blue) curves:  $e'_g$  states;  $E_F = 0$ .

and the empty  $e'_g$  bands, in agreement with Ref. [24]. The hole doped system, on the other hand, is metallic, with conduction states stemming from both  $a_g$  and  $e'_g$  bands. If we associate the peak near  $E_F$  with coherent states, the large peak at 1.1 eV binding energy, i.e., below the bottom of the LDA density of states, represents the incoherent weight related to the lower Hubbard band. It has mainly  $a_g$  character, with weak  $e'_g$  admixture. The position of this feature is in good agreement with the photoemission spectra for  $\text{La}_{0.95}\text{Sr}_{0.05}\text{TiO}_3$  [3]. Moreover, the ratio between incoherent and coherent weight is roughly 3 : 1. This is also consistent with the photoemission data which reveal substantially more incoherent than coherent emission.

In summary, we have shown that multi-band ED DMFT is a powerful method to study the subtle interorbital charge rearrangement triggered by the density-driven Mott transition in  $\text{La}_{1-x}\text{Sr}_x\text{TiO}_3$ . In particular,

we have shown that doping with Sr gives rise to a first-order insulator to metal transition that is accompanied by a significant orbital depolarization. Injection of only a few percent of holes into the Ti  $t_{2g}$  bands leads to a much larger simultaneous electron and hole doping of different subbands. The transition exhibits separation between insulating and metallic phases. In the latter, subband charge compressibilities are very large and have opposite signs. Moreover, electron doping generates an internal charge flow in the same direction as hole doping. Since other Mott insulators such as  $\text{V}_2\text{O}_3$  and  $\text{Ca}_{2-x}\text{Sr}_x\text{RuO}_4$  also exhibit nearly complete orbital polarization, it is likely that doping these systems with electron or hole donors will lead to a similar enhancement of orbital fluctuations as discussed here for  $\text{La}_{1-x}\text{Sr}_x\text{TiO}_3$ .

I like to thank Eva Pavarini for the density of states distributions shown in Fig. 1, and Theo Costi for useful discussions.

- 
- [1] M. Imada, A. Fujimori, and Y. Tokura, *Rev. Mod. Phys.* **70**, 1039 (1999).
- [2] K. Kumagai *et al.*, *Phys. Rev. B* **48**, 7836 (1993).
- [3] T. Yoshida *et al.*, *EuroPhys. Lett.* **59**, 258 (2002).
- [4] N. Furukawa and M. Imada, *J. Phys. Soc. Japan* **60**, 3604 (1991).
- [5] The Pruschke, D. L. Cox, and M. Jarrell, *Phys. Rev. B* **47**, 3553 (1993).
- [6] D. S. Fisher, G. Kotliar, and G. Moeller, *Phys. Rev. B* **52**, 17112 (1995).
- [7] G. Kotliar, S. Murthy, and M. J. Rozenberg, *Phys. Rev. Lett.* **89**, 046491 (2002).
- [8] Y. Ono, R. Bulla, A. Hewson, and M. Potthoff, *Eur. Phys. J. B* **22**, 283 (2002).
- [9] A. Camjayi, R. Chitra, and M. J. Rozenberg, *Phys. Rev. B* **73**, 041103 (2006).
- [10] A. Macridin, M. Jarrell, and T. Maier, *Phys. Rev. B* **74**, 085104 (2006).
- [11] Ph. Werner and A. J. Millis, *Phys. Rev. B* **75**, 085108 (2007).
- [12] D. J. Garca, E. Miranda, K. Hallberg, and M. J. Rozenberg, *Phys. Rev. B* **75**, 121102(R) (2007).
- [13] M. Eckstein, M. Kollar, M. Potthoff, and D. Vollhardt, *Phys. Rev. B* **75**, 125103 (2007).
- [14] M. B. Zolf, T. Pruschke, J. Keller, A. I. Poteryaev, I. A. Nekrasov, and V. I. Anisimov, *Phys. Rev. B* **61** 12810 (2000).
- [15] I. A. Nekrasov, K. Held, N. Blumer, A. I. Poteryaev, V. I. Anisimov, and D. Vollhardt, *Eur. Phys. J. B* **18** 55 (2000).
- [16] V. S. Oudovenko, G. Palsson, S. Y. Savrasov, K. Haule, and G. Kotliar, *Phys. Rev. B* **70**, 125112 (2004).
- [17] L. Craco, M. S. Laad, S. Leoni, and E. Muller-Hartmann, *Phys. Rev. B* **70**, 195116 (2004).
- [18] E. Pavarini, S. Biermann, A. Poteryaev, A. I. Lichtenstein, A. Georges, and O. K. Andersen, *Phys. Rev. Lett.* **92**, 176403 (2004).
- [19] G. Keller, K. Held, V. Eyert, D. Vollhardt, and V. I. Anisimov, *Phys. Rev. B* **70**, 205116 (2004).
- [20] A. I. Poteryaev, J. M. Tomczak, S. Biermann, A. Georges, A. I. Lichtenstein, A. N. Rubtsov, T. Saha-Dasgupta, and O. K. Andersen cond-mat/0701263.
- [21] A. Liebsch and H. Ishida, *Phys. Rev. Lett.* **98**, 216404 (2007).
- [22] C. A. Perroni, H. Ishida, and A. Liebsch, *Phys. Rev. B* **75**, 045125 (2007). See also: A. Liebsch, *Phys. Rev. Lett.* **95**, 116402 (2005); A. Liebsch and T. A. Costi, *Eur. Phys. J.* **51**, 523 (2006).
- [23] A. Liebsch and H. Ishida, cond-mat/0705.3627; A. Liebsch, to be published.
- [24] E. Pavarini, A. Yamasaki, J. Nuss, and O. K. Andersen, *New J. Phys.* **7**, 188 (2005).
- [25] M. Cwik *et al.*, *Phys. Rev. B* **68**, 060401 (2003); see also: J. Hemberger *et al.*, *Phys. Rev. Lett.* **91**, 066403 (2003).
- [26] H. W. Haverkort *et al.*, *Phys. Rev. Lett.* **94**, 056401 (2005).
- [27] Th. Pruschke, M. Jarrell, and J. K. Freericks, *Adv. Phys.* **44**, 187 (1995).
- [28] A. Georges, G. Kotliar, W. Krauth and M. J. Rozenberg, *Rev. Mod. Phys.* **68**, 13 (1996).
- [29] G. Kotliar, S. Y. Savrasov, K. Haule, V. S. Oudovenko, O. Parcollet, and C. A. Marianetti, *Rev. Mod. Phys.* **78**, 865 (2006).
- [30] G. Kotliar and D. Vollhardt, *Phys. Today* **57**(3), 53 (2004).
- [31] M. Caffarel and W. Krauth, *Phys. Rev. Lett.* **72**, 1545 (1994).
- [32] R. B. Lehoucq, D. C. Sorensen, and C. Yang, *ARPACK Users' Guide* (1997).
- [33] In contrast, in Ref. [17] orbital polarization was found to slightly decrease in the insulating phase.